Journal of Interfaces, Thin films, and Low dimensional systems 5 (2) Winter and Spring (2022) 525-535

Entanglement, QFI and squeezing of hybrid state in non-inertial frame

Scientific research paper

Seyedeh Robabeh Miry*, Fatemeh Ahmadi

Department of Engineering Sciences and Physics, Buein Zahra Technical University, Buein Zahra, Qazvin, Iran

ARTICLE INFO

Article history:
Received 24 June 2022
Revised 4 October 2022
Accepted 8 February 2023
Available online 22 April 2023

Keywords
Entanglement
Two-mode squeezing
Quantum Fisher information
Rindler coordinate

ABSTRACT

We study the effect of acceleration of the observer on the quantum Fisher information and entanglement using hybrid state. The two-partite entangled hybrid state is consisted of discrete (vacuum and single photon) and continues (coherent) variable states. When one of the observers (e.g., Rob) is uniformly accelerated with respect to the other partner, Alice, we find that quantum Fisher information has a more stable structure than entanglement. Results show that quantum Fisher information decreases with the increase of the acceleration but remains finite in the limit of infinite acceleration that is in contrast with entanglement. Moreover, the effect of acceleration is investigated on the value of two-mode squeezing.

1 Introduction

Quantum information science is based on the discovery of the characteristics of the quantum system which enables tasks that cannot be accomplished in a classical world. Entanglement plays a central role in quantum information theory and is considered as a resource for quantum communication and teleportation [1]. Attention to the theory of relativistic quantum information has increased over the past decade. Understanding entanglement in relativistic settings has been a key question in relativistic quantum information. At the beginning of this theory, entanglement was considered in an inertial frame [2, 3]. Moreover, many articles investigated the invariance of entanglement under the Unruh effect when observers are in uniform acceleration [4, 5, 6].

There are many programs in which satellites are used to distribute entanglement in quantum processes such as cryptography and teleportation [7]. Relative effects are important in places where satellites work [8, 9]. Therefore, a full understanding of the effects of relativity on quantum properties allows us to correct and improve the methods of quantum information theory by considering these effects.

Recently, quantum Fisher information (QFI) [10] has attracted considerable attention, due to its own significance in quantum estimation and quantum information theory [11]. QFI is an indicator of the evolution speed of the quantum state and the inverse of this measure determines the achievable precision in parameter estimation. According to this ability, QFI plays a significant role in the field of quantum metrology [12] and multi-partite entanglement detection [13, 14]. QFI can quantify the teleportation of specific parameters encoded in quantum states accurately [15]. In this regard, the evolution of the teleportation of quantum resources and QFI under the Unruh effect has been studied in [16, 17, 18].

Moreover, squeezed states of light have significant applications in several branches of quantum information

*Corresponding author.
Email address: Zahramiry@bzte.ac.ir
DOI: 10.22051/jitl.2023.42294.1079

processing [19, 20, 21]. The state is known as a squeezed state if its quantum fluctuation in one of the field quadratures becomes less than that of the vacuum state or canonical coherent state [22, 23]. One of the most important applications of the squeezed state is in the field of interferometric techniques to detect very weak forces such as gravitational waves [24]. In this context, it is shown that frequency-dependent squeezing can improve the force sensitivity of the optomechanical interferometer [25]. Furthermore, the enhancement of spectroscopy of the rubidium atomic ensemble has been proved by using the polarization squeezed state [26]. On the other hand, it is shown that the squeezed single-photon state can be used as a resource for the teleportation of coherent state qubits [27].

To improve quantum technologies, different states have been used. There are several studies that have investigated the properties of discrete variable entangled states such as Bell states [2, 4, 5, 6].

Moreover, there are few studies on the entanglement properties of continuous variable entangled systems. The theory of continuous-variable entanglement with special emphasis on foundational aspects, conceptual structures, and mathematical methods has been considered in some works [28, 29].

Furthermore, in some practical implementations, the two subsystems can differ in their nature, for example, an electromagnetic field and a matter system, or in the way they are most conveniently described, for example, in a discrete- and continuous-variable framework [30]. Considering the practical importance of these systems, we refer to the hybrid entangled state which is a combination of discrete and continuous variable states. This mentioned state is useful for quantum swapping [31], and super-dense coding [32]. In this regard, it is shown that by applying the hybrid entanglement, perfect quantum teleportation is possible [33]. So, a quantitative understanding of entanglement, QFI, and squeezing of hybrid states in non-inertial frames are required for quantum information processing tasks using hybrid states.

The remainder of this paper is organized as follows. In section 2, we consider the parametrized hybrid entangled state. In section 3, we review the non-inertial frame and introduce the Rindler coordinate and the Unruh effect for scalar particles as experienced by the accelerated observer. In section 4 we discuss the effect of the Unruh noise on the QFI of the parameterized arbitrary hybrid state. To quantify the value of entanglement of the hybrid state, we find the concurrence of the hybrid state in the inertial and non-inertial frame in section 5. In section 6, we study the behavior of the squeezing of hybrid state. Finally, the summary and conclusions are given in section 7.

2 The suggested model

Here, we consider a free scalar field which is, from an inertial perspective, in a hybrid state. The hybrid state can be produced in the lab and exploited for any current realization of bipartite quantum information with continuous and discrete variables [34, 35]. It belongs to the class of states, which is possible to characterize the redistribution of correlations due to relativistic effects. So, we focus on the parameterized (and arbitrary) hybrid state as the combination of vacuum and single-photon states with the coherent state which can be described as

$$|\psi\rangle^{in} = \cos\theta\,|\alpha\rangle_A|0\rangle_R + \sin\theta\,e^{i\phi}|-\alpha\rangle_A|1\rangle_R, \quad (1)$$

where θ and ϕ refer to the polar and azimuth angles on the Bloch sphere such that $0 \le \theta \le \pi/2$ and $0 \le \phi \le \pi$. On the other hand, the subscripts A and R indicate the modes associated with the observers Alice and Rob, respectively, and coherent states $|\alpha\rangle$ and $|-\alpha\rangle$ are defined as [36, 37, 38]

$$|\alpha\rangle = e^{-\frac{|\alpha|^2}{2}}\sum_{l=0}^{\infty}\frac{\alpha^l}{\sqrt{l!}}|l\rangle,$$

$$\left|-\alpha\rangle = e^{-\frac{|\alpha|^2}{2}}\sum_{l=0}^{\infty}\frac{(-\alpha)^l}{\sqrt{l!}}\right|l\rangle. \quad (2)$$

Since the coherent states, $|\alpha\rangle$ and $|-\alpha\rangle$, are non-orthogonal, it is more convenient to consider the even and odd coherent states defined as

$$|+\rangle = \mathcal{N}_+(|\alpha\rangle + |-\alpha\rangle)$$

$$|-\rangle = \mathcal{N}_-(|\alpha\rangle - |-\alpha\rangle), \quad (3)$$

where $\mathcal{N}_\pm = [2(1 \pm e^{-2|\alpha|^2})]^{-\frac{1}{2}}$. So, instead of working with $|\alpha\rangle$ and $|-\alpha\rangle$, we use the following relation

$$|\pm\alpha\rangle = \frac{1}{2}\left[\frac{|+\rangle}{\mathcal{N}_+} \pm \frac{|-\rangle}{\mathcal{N}_-}\right]. \quad (4)$$

3 Non-inertial frames: the Unruh effect

Considering a free scalar field in 3 + 1 dimensions, the Klein-Gordon equation takes the following form

$$(\partial_t^2 - \partial_x^2)\phi = 0, \quad (5)$$

in Minkowski coordinates (t, x). The quantized scalar field, ϕ, can be expressed

as

$$\phi(t,x) = \frac{1}{\sqrt{2\pi}}\int \frac{dk}{\sqrt{2|k|}}\left(e^{-i|k|t+ikx}a_k + e^{i|k|t-ikx}a_k^\dagger\right), \quad (6)$$

where the creation and annihilation operators follow the appropriate commutation relations $[a_k, a_k^\dagger] = \delta_{k\acute{k}}$ and describe particles moving with momentum k either in the positive x direction $(k > 0)$ or in the negative x direction $(k < 0)$. The vacuum state in the laboratory frame (the Minkowski vacuum) is defined as $a_k|0\rangle = 0$.

Now, we consider an inertial observer, named Alice, who has a detector sensitive to modes A, and another observer, Rob, who moves with uniform acceleration, a, and has a detector sensitive to modes B. For studying the entanglement from the point of view of an accelerated observer we need to find field quantization in non-inertial frames.

The appropriate coordinates for accelerated observers are (τ, ξ) known as Rindler coordinates. Two different sets of Rindler coordinates are necessary for covering the Minkowski space. These sets of coordinates define two Rindler regions that are causally disconnected from each other,

$$t(\tau,\xi) = a^{-1}e^{a\xi}\sinh a\tau$$
$$x(\tau,\xi) = a^{-1}e^{a\xi}\cosh a\tau, \quad (7)$$

In region I and

$$t(\tau,\xi) = -a^{-1}e^{a\xi}\sinh a\tau$$
$$x(\tau,\xi) = -a^{-1}e^{a\xi}\cosh a\tau, \quad (8)$$

in region II, where a denotes Rob's proper acceleration. The set of Eqs. (7) and (8) both give rise to the same Rindler metric as

$$ds^2 = dt^2 - dz^2 - dx_\perp^2 = e^{2a\xi}(d\tau^2 - d\xi^2) - dx_\perp^2, \quad (9)$$

where $x_\perp$ are the same in both Minkowski and Rindler space times. A particle undergoing uniform acceleration remains constrained to either of the Rindler regions I or II having no access to the opposite region, since these two regions are causally disconnected (see Fig. 1).

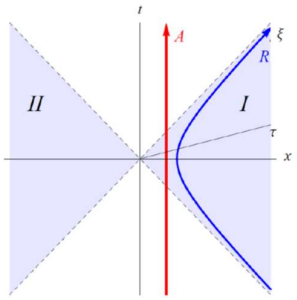

Figure 1: Sketch of the world lines for the inertial observer Alice and the accelerated observer Rob. The set (t, x) denotes Minkowski coordinates, while the set (τ, ξ) denotes Rindler coordinates. The causally disconnected Rindler regions *I* and *II* are evidenced.

The mode expansion in the accelerated frame is quite similar to Eq. (6) as

$$\phi(\tau,\xi) = \frac{1}{\sqrt{2\pi}}\int \frac{dk}{\sqrt{2|k|}}\left(e^{-i|k|\tau+ik\xi}b_k + e^{i|k|\tau-ik\xi}b_k^\dagger\right). \quad (10)$$

The vacuum state in the accelerated frame (the Rindler vacuum) is defined as $b_k|0\rangle = 0$. Although the operators $a_k, a_k^\dagger$ and $b_k, b_k^\dagger$ satisfy similar commutation relations, they are different. So, the Rindler vacuum and the Minkowski vacuum are two different quantum states of the field. The relation between $a_k, a_k^\dagger$ and $b_k, b_k^\dagger$ is given by the Bogolyubov transformation as $a = \cosh r\, b_I - \sinh r\, b_{II}^\dagger$ [39]. We find the Minkowski vacuum in terms of Rindler states as

$$|0_k\rangle = \frac{1}{\cosh r}\sum_n \tanh^n r\,|n_k\rangle_I|n_k\rangle_{II}, \tag{11}$$

where $|n_k\rangle_I$ and $|n_k\rangle_{II}$ denote the mode decomposition in regions I and II respectively, and $\cosh r = (1-e^{-2\pi\Omega})^{-\frac{1}{2}}$ with $\Omega = \frac{|k|c}{a}$. In this regard, one particle state can be obtained as follows

$$\begin{aligned} a_k^\dagger|0_k\rangle &= |1_k\rangle \\ &= \frac{1}{\cosh^2 r}\sum_n \tanh^n r\sqrt{n+1}|(n \\ &\quad + 1)_k\rangle_I|n_k\rangle_{II}. \end{aligned} \tag{12}$$

For clarifying the Unruh effect, we find the mean density of particles, the expectation value of $\langle N\rangle \equiv \langle 0|b_k^\dagger b_k|0\rangle$, in the Ω mode. We notice that $|0\rangle$ is the Minkowski vacuum. With calculating $\langle N\rangle$, one can find the density of b-particles in a-vacuum as $n_\Omega = \frac{1}{\exp(\frac{2\pi\Omega}{a}-1)}$. The energy of e massless particle with momentum Ω is equal to $E = |\Omega|$. So, this relation is equivalent to the Bose-Einstein distribution $n(E) = \frac{1}{\exp(\frac{E}{T}-1)}$, if we define $T \equiv \frac{a}{2\pi}$ as the Unruh temperature. So, an accelerated detector behaves as though it were placed in a thermal bath with temperature T. This is the Unruh effect.

Now, assume that Alice and Rob initially share the state (1), and then Rob undergoes uniform acceleration a. Using Eqs. (11) and (12), this situation can be expressed with the following quantum state

$$\begin{aligned} &|\psi\rangle_{AR_{I,II}} \\ &= \frac{\cos\theta}{\cosh r}|\alpha\rangle_A\sum_n \tanh^n r\,|n_k\rangle_I|n_k\rangle_{II} \\ &+ \frac{\sin\theta\, e^{i\phi}}{\cosh^2 r}|-\alpha\rangle_A \\ &\times \sum_n \tanh^n r\sqrt{n+1}|(n+1)_k\rangle_I|n_k\rangle_{II} \\ &= \frac{\cos\theta}{2\cosh r}\left[\frac{|+\rangle}{\mathcal{N}_+}+\frac{|-\rangle}{\mathcal{N}_-}\right] \\ &\times \sum_n \tanh^n r\,|n_k\rangle_I|n_k\rangle_{II} \\ &\quad + \frac{\sin\theta}{2\cosh^2 r}\left[\frac{|+\rangle}{\mathcal{N}_+}-\frac{|-\rangle}{\mathcal{N}_-}\right] \\ &\times \sum_n \tanh^n r\sqrt{n+1}|(n+1)_k\rangle_I|n_k\rangle_{II}. \end{aligned} \tag{13}$$

Tracing over the causally disconnected Region II, one can obtain the reduced density matrix as

$$\begin{aligned} &\rho_{AR_I} \\ &= \frac{\cos^2\theta}{4\cosh^2 r}\left[\frac{|+\rangle}{\mathcal{N}_+}+\frac{|-\rangle}{\mathcal{N}_-}\right]\left[\frac{\langle+|}{\mathcal{N}_+}+\frac{\langle-|}{\mathcal{N}_-}\right] \\ &\times \sum_n tanh^n r\,|n_k\rangle\langle n_k| \\ &\quad + \frac{\sin\theta\cos\theta}{4\cosh^3 r}\sum_n \tanh^{2n} r\sqrt{n+1} \\ &\times (e^{-i}\left[\frac{|+\rangle}{\mathcal{N}_+}+\frac{|-\rangle}{\mathcal{N}_-}\right]\left[\frac{\langle+|}{\mathcal{N}_+}-\frac{\langle-|}{\mathcal{N}_-}\right] \\ &\times |n_k\rangle\langle(n+1)_k| + H.C) \\ &+ \frac{\sin^2\theta}{4\cosh^4 r}\left[\frac{|+\rangle}{\mathcal{N}_+}-\frac{|-\rangle}{\mathcal{N}_-}\right]\left[\frac{\langle+|}{\mathcal{N}_+}-\frac{\langle-|}{\mathcal{N}_-}\right] \\ &\times \sum_n \tanh^{2n} r\,(n+1) \\ &\times |(n+1)_k\rangle\langle(n+1)_k|, \end{aligned} \tag{14}$$

where $|\pm,n\rangle = |\pm_A\rangle|n_R\rangle_I$, and the orthogonal basis (Eq. (3)) are used.

4 Quantum Fisher Information of Hybrid State in Non-inertial Frame

In the field of quantum information processing, parameter estimation is a basic task. In quantum metrology, physical quantum Fisher information is used to describe the ultimate precision that can be achieved by a general parameter estimation experiment.

Consider an N-dimensional quantum state ρ_λ on an unknown parameter λ. If we intend to extract

information about λ from ρ_λ, a set of quantum measurement $E(\xi)$ should be performed. According to classical theory, the quantity of any measurement can be specified by a form of information called Fisher information. The quantum Fisher information can be written as [40, 41]

$$F = \sum_{i=1}^{m} \frac{(\dot{p_i})^2}{p_i} + \sum_{i=1}^{m} 4p_i F_{\lambda i} - \sum_{i\neq j}^{m} \frac{8p_i p_j}{p_i + p_j} \left|\langle \psi_i | \dot{\psi_j} \rangle\right|^2, \quad (15)$$

where $\dot{p_i} = \partial_\lambda p_i$, $|\dot{\psi_j}\rangle = |\partial_\lambda \psi_j\rangle$ and $F_{\lambda i} = \langle \partial_\lambda \psi_i | \partial_\lambda \psi_i \rangle - |\langle \psi_i | \partial_\lambda \psi_i \rangle|^2$. From expression (15), one can identify that the QFI can be divided into three parts: the first term is just the classical contribution if we regard the set of nonzero eigenvalues as a probability distribution; the second term is a weighted average over all pure-state QFI; the last term stems from the mixture of pure states and thus decreases the total QFI. Now, we return to the state of the system which is prepared in the hybrid state in an inertial frame as (1). The related density matrix has the following expression

$$\begin{aligned}
&\rho_{AR} \\
&= \frac{\cos^2\theta}{4}\left[\frac{|+\rangle}{\mathcal{N}_+} + \frac{|-\rangle}{\mathcal{N}_-}\right]\left[\frac{\langle +|}{\mathcal{N}_+} + \frac{\langle -|}{\mathcal{N}_-}\right]|0\rangle\langle 0| \\
&+ \frac{\cos\theta \sin\theta}{4} \\
&\times \left(e^{-i\phi}\left[\frac{|+\rangle}{\mathcal{N}_+} + \frac{|-\rangle}{\mathcal{N}_-}\right]\left[\frac{\langle +|}{\mathcal{N}_+} - \frac{\langle -|}{\mathcal{N}_-}\right]|0\rangle\langle 1| + H.C\right) \\
&+ \frac{\sin^2\theta}{4}\left[\frac{|+\rangle}{\mathcal{N}_+} - \frac{|-\rangle}{\mathcal{N}_-}\right]\left[\frac{\langle +|}{\mathcal{N}_+} - \frac{\langle -|}{\mathcal{N}_-}\right]|1\rangle\langle 1|, \quad (16)
\end{aligned}$$

which has the non-zero eigenvalue equal to $\lambda = 1$ and eigenvector as

$$\begin{aligned}
&-\frac{1}{\sqrt{2}}[e^{-i\phi}\cos\theta\sqrt{1+e^{-2|\alpha|^2}}, \\
&e^{-i\phi}\cos\theta\sqrt{1-e^{-2|\alpha|^2}}, \\
&\sin\theta\sqrt{1+e^{-2|\alpha|^2}}, -\sin\theta\sqrt{1-e^{-2|\alpha|^2}}]. \quad (17)
\end{aligned}$$

We find the QFI with respect to θ, F_θ, and ϕ, F_ϕ as

$$F_\theta = 4,\ F_\phi = \sin^2 2\theta, \quad (18)$$

which shows that F_θ does not depend on ϕ and is constant. The QFI of ϕ depends on the value of θ. In addition, F_θ and F_ϕ are irrespective of α, the hybrid parameter.

We assume that Alice is stationary and has a detector sensitive only to mode A. Rob moves with uniform acceleration and takes with him a detector that only detects particles corresponding to mode R. We are going to answer this question; what is the QFI when Rob undergoes uniform acceleration.

First, we consider the QFI associated with θ. In order to achieve this aim, we take the reduced density matrix (Eq. (14)) which its non-zero eigenvalue for the definite value of n is

$$\begin{aligned}
&\lambda_n = \frac{\tanh^{2n} r}{\cosh^2 r}\lambda_n^0, \\
&\lambda_n^0 = \left(\cos^2\theta + \frac{(n+1)\sin^2\theta}{\cosh^2 r}\right), \quad (19)
\end{aligned}$$

and its normalized corresponding eigenvector is given by

$$\begin{aligned}
&-\frac{1}{\sqrt{2\lambda_n^0}}[e^{-i\phi}\cos\theta\sqrt{1-e^{-2|\alpha|^2}}, \\
&e^{-i\phi}\cos\theta\sqrt{1+e^{-2|\alpha|^2}}, \\
&\sin\theta\sqrt{1-e^{-2|\alpha|^2}}\frac{\sqrt{n+1}}{\cosh r}, \\
&-\sin\theta\sqrt{1+e^{-2|\alpha|^2}}\frac{\sqrt{n+1}}{\cosh r}]. \quad (20)
\end{aligned}$$

Using Eq. (15) we find that F_θ is invariant, that is $F_\theta = 4$ independent of the acceleration parameter r. It means that the QFI about θ is unaffected under the effect of the Unruh channel. On the other hand, we find for F_ϕ

$$F_\phi = \frac{4\cos^2\theta\sin^2\theta}{\cosh^4 r}\sum_n \frac{(n+1)\tanh^{2n} r}{\lambda_n^0}. \quad (21)$$

As we see, the QFI of F_θ and F_ϕ is irrespective of the hybrid parameter, α and have no ϕ dependence. Moreover, The QFI with respect to the parameters θ and F_θ, is independent of the state parameter θ while the QFI with respect to the parameters ϕ and F_ϕ is state-dependent and depends upon θ. Figure 2 shows the r -dependence graph of F_ϕ for a series value of θ. One can check that $\lim_{r\to 0} F_\phi = sin^2 2\theta$ is consistent with the initial value. As the acceleration r increases, F_ϕ gradually decreases and converges to a non-zero value in the limit of infinite acceleration. This is consistent with the fact that the Unruh acceleration produces a thermal-like effect. The QFI provides a lower bound on the error of an estimation. So, quantum estimation would be expected not to increase with the increase of temperature.

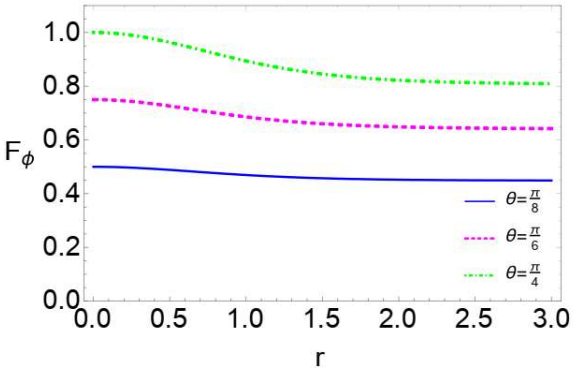

Figure 2. The graph of $F_\phi$as a function of r and certain values of θ for hybrid state in non-inertial motion. The continuous (blue) line is plotted for $\theta = \frac{\pi}{8}$, the dashed (magenta) line is plotted for $\theta = \frac{\pi}{6}$, and the dotted (green) line is plotted for $\theta = \frac{\pi}{4}$.

5 Concurrence

In this section, we study the dependence of the entanglement of the state (Eq. (1)), on the acceleration of the observer. To find out the behavior of entanglement, we use the concurrence as a measure of entanglement which is defined as [1]

$$C = 2\max(0, \sqrt{\lambda_1} - \sqrt{\lambda_2} - \sqrt{\lambda_3} - \sqrt{\lambda_4}), \quad (22)$$

where $\lambda_i (i = 1,2,3,4)$ are eigenvalues of the density matrix operator $\rho\tilde{\rho}$ in decreasing order. The density operator $\tilde{\rho}$ is defined as $\tilde{\rho} = (\sigma_y \otimes \sigma_y)\rho^*(\sigma_y \otimes \sigma_y)$ where ρ^* is the complex conjugate of ρ and σ_y is the Pauli matrix. The nonzero values of the concurrence indicates that the subsystems are entangled.

First, we assume that Alice and Rob are in the inertial frame. Considering the density matrix (Eq. (16)), one can find the concurrence as

$$C = 2\cos\theta\sin\theta\sqrt{1 - e^{-4|\alpha|^2}}, \quad (23)$$

Figure 3 shows the concurrence against θ and some values of α. As we expect, the maximum correlation between subsystems takes places around $\theta = \frac{\pi}{4}$ and has a symmetry with respect to $\theta = \frac{\pi}{4}$.

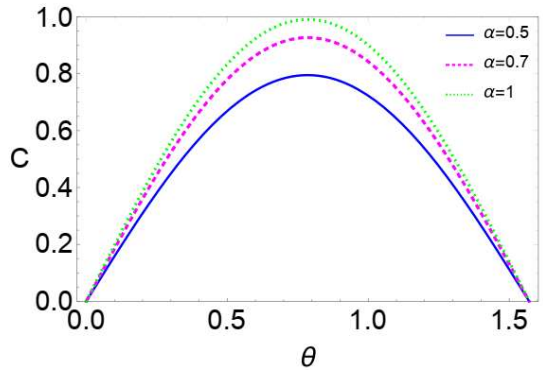

Figure 3: The graph of concurrence against θ and various values of α. The continuous (blue) line is plotted for $\alpha = 0.5$, the dashed (magenta) line is plotted for $\alpha = 0.7$ and the dotted (green) line is plotted for $\alpha = 1$.

Now, we study the behavior of entanglement in the situation that Rob has uniform acceleration and Alice remains stationary. Using the reduced density matrix (Eq. (14)), the concurrence can be obtained as follows

$$C = \frac{2\cos\theta\sin\theta}{\cosh^3 r} \times \sqrt{(1 - e^{-4|\alpha|^2})\sum_{n=0}^{\infty} \tanh^{4n} r\,(n+1)}. \quad (24)$$

The concurrence of the system with accelerated motion has been plotted in terms of r and various values of θ in figure 3. The figure illustrates that, when the parameter r increases, the entanglement decreases, and ultimately in enough large values of r the correlation between subsystems will be removed, completely.

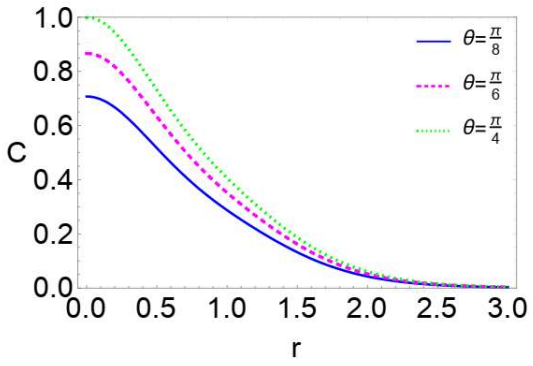

Figure 4: The graph of concurrence against acceleration parameter r and various values of θ. The continuous (blue) line is plotted for $\theta = \frac{\pi}{8}$, the dashed (magenta) line is plotted for $\theta = \frac{\pi}{6}$ and the dotted (green) line is plotted for $\theta = \frac{\pi}{4}$. We set $\alpha = 3$.

6 Squeezing

The squeezing phenomenon occurs when the quantum fluctuation in one of the field quadratures takes the value below the value of vacuum or canonical coherent states. In order to investigate the squeezing of the two-mode entangled hybrid state, we consider the two-mode quadrature operators as

$$\hat{X} = \frac{\hat{a} + \hat{a}^\dagger + \hat{b} + \hat{b}^\dagger}{2\sqrt{2}}, \hat{Y} = \frac{\hat{a} - \hat{a}^\dagger + \hat{b} - \hat{b}^\dagger}{2i\sqrt{2}}, \quad (25)$$

that obey the commutation relation

$$[\hat{X}, \hat{Y}] = \frac{i}{2} \quad (26)$$

The uncertainty relation for these operators is given by $(\Delta\hat{X})^2(\Delta\hat{Y})^2 \geq \frac{1}{4}$, where $(\Delta\hat{X})^2 = \langle\hat{X}^2\rangle - \langle\hat{X}\rangle^2$ and $(\Delta\hat{Y})^2 = \langle\hat{Y}^2\rangle - \langle\hat{Y}\rangle^2$. The state is called two-mode squeezed state respect to $\hat{X}$ or $\hat{Y}$ component, if the parameters

$$S_X = 4(\Delta\hat{X})^2 - 1, S_Y = 4(\Delta\hat{Y})^2 - 1, \quad (27)$$

satisfy the inequalities $-1 < S_X < 0$ or $-1 < S_Y < 0$.

However, it is noteworthy that, if one quadrature has less noise than a coherent state or a vacuum state, the fluctuations in the other quadrature must be enhanced until the uncertainty relation is preserved. According to this point, one of the S_X or S_Y parameters in Eq. (27) can take negative values.

In the following, the existence of squeezing is studied in two cases: inertial and non-inertial motions. At first, we consider the system in the inertial motion in which the subsystems have no acceleration relative to each other. In this situation, for the hybrid state (Eq. (1)), the following relations are obtained

$$\langle\hat{X}\rangle = \frac{1}{2\sqrt{2}}\left((\cos^2\theta - \sin^2\theta)(\alpha + \alpha^*)\right.$$
$$\left. + \cos\theta\sin\theta e^{-2|\alpha|^2}(e^{i\phi} + e^{-i\phi})\right), \quad (28)$$

$$\langle\hat{X}^2\rangle = \frac{1}{8}(\alpha^2 + \alpha^{*2} + 2|\alpha|^2 + +2sin^2\theta$$
$$+ 2\cos\theta\sin\theta \times e^{-2|\alpha|^2}((\alpha + \alpha^*)e^{i\phi} + (\alpha - \alpha^*)e^{-i\phi})). \quad (29)$$

Using Eqs. (27)-(29), S_X is plotted against α and various values of θ in Fig. 5. As it is obvious, the parameter S_X takes negative values for small values of θ, and α. So, the hybrid state behaves as a two-mode squeezed state.

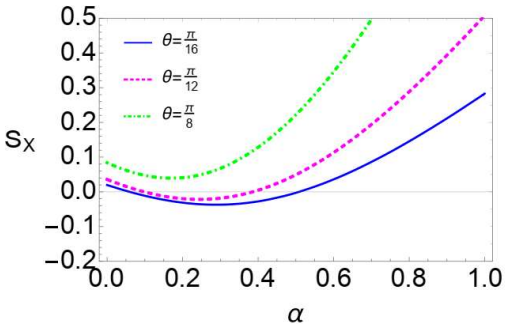

Figure 5: The graph of S_X as a function of α and certain values of θ for hybrid state in the inertial motion. We set $\phi = 0$. The continuous (blue) line is plotted for $\theta = \frac{\pi}{16}$. , the dashed (magenta) line is plotted for $\theta = \frac{\pi}{12}$. and the dotted (green) line is plotted for $\theta = \frac{\pi}{8}$.

Now, we extend the studies to the non-inertial motion in which Rob has uniform acceleration. By applying the

expression of the hybrid state in the non-inertial frame (Eq. (13)), one can obtain

$$\langle \hat{X} \rangle = \frac{1}{2\sqrt{2}}\left((\cos^2\theta - \sin^2\theta)(\alpha + \alpha^*) + \cos\theta\sin\theta\cosh r\, e^{-2|\alpha|^2}(e^{i\phi} + e^{-i\phi})\right). \quad (30)$$

$$\langle \hat{X}^2 \rangle = \frac{1}{8}(\alpha^2 + \alpha^{*2} + 2|\alpha|^2 + 2 + 2\sin^2\theta(2\cosh^2 r - 1) + 2\cos^2\theta(2\cosh^2 r - 1) + 2\cos\theta\sin\theta\cosh r \times e^{-2|\alpha|^2}((\alpha + \alpha^*)e^{i\phi} + (\alpha - \alpha^*)e^{-i\phi})). \quad (31)$$

The behavior of S_X for different values of the acceleration parameter r has been plotted in Fig. 6. The figure displays that for small values of the parameter r, the hybrid state remains in the squeezed state. However, with increasing the parameter r, the depth of the squeezing decreases until for values around $r = 0.2$ before it completely disappears. Therefore, the two-mode squeezing between subsystems has been degraded by the Unruh effect in non-inertial frames.

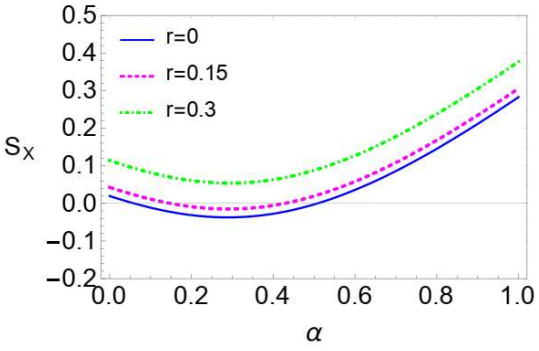

Figure 6: The graph of S_X as a function of α and certain values of r for the hybrid state in non-inertial motion. We set $\phi = 0$. The continuous (blue) line is plotted for $r = 0$, the dashed (magenta) line for $r = 0.15$, and the dotted (green) line is plotted for $r = 0.3$.

7 Conclusions

In this paper, we have studied the behavior of the system that is prepared in the two-mode entangled hybrid state where one of the subsystems is uniformly accelerated. We considered parametrized states, where the α parameter is introduced to describe coherent states of the hybrid state, and the weight parameter θ and phase parameter ϕ are introduced to two-mode entangled states. We consider that Alice and Rob each share one mode of the state and then Rob is uniformly accelerated. At first, we computed the quantum fisher information of the system when Rob is uniformly accelerated. We found that the QFI of θ, F_θ, remains invariant and does not change with the accelerated parameter r while the QFI of ϕ, F_ϕ, decreases with increasing acceleration. It is remarkable that for large values of r, F_ϕ reaches non-zero values.

In continuation, we investigated the behavior of the entanglement by using the concurrence measure. The results indicated that the concurrence decreases with increasing the acceleration parameter r, and for enough large values of r tends to zero. So, comparing the QFI and concurrence, QFI has a more subtle physical structure than concurrence. Finally, we have studied the variation of the two-mode squeezing of the hybrid state. When both observers are in the inertial frame, the hybrid state is a two-mode squeezed state for small values of θ and α. While Rob accelerates uniformly, the width and depth of two-mode squeezing decrease and disappear for large values of r.

In summary, properties of the entangled hybrid state have been investigated in a non-inertial frame. Due to the obtained results, we found that the degree of entanglement of the hybrid state decreases with increasing the acceleration parameter r. Nevertheless, the hybrid state for small values of the acceleration parameter r, is still an entangled state and can be used for quantum information processing tasks.

The obtained results for QFI indicated that the estimation of parameter θ is not affected by the acceleration of the system. But, the accuracy of the estimation of parameter ϕ decreases slightly with increasing acceleration. Therefore, the hybrid entangled state in the non-inertial frame is still a suitable quantum state in the field of quantum metrology [12]

Our results can be used experimentally in free-space quantum experiments. Particularly, consider a quantum mechanical system consisting of two entangled photons.

One photon of each pair is detected on the ground while the other is sent to the International Space Station (ISS). Different theoretical models have been proposed to analyze this scenario with widely varying results [42, 43]. Understanding the entanglement of a hybrid state, composed of the coherent state which is treated as a semiclassical state, and the vacuum and single-photon states that are successfully demonstrated in recent experiments [34, 35], plays an important role in these experiments [44]. As a relevant example, space-based quantum clocks allow for the distribution and synchronization of timing information and promise performance upgrades of existing global navigation satellite systems (GNSS). These clocks also enable distributed quantum information processing such as faster algorithmic processing of data through distributed quantum computing [45].

Our results are on one hand an interesting application of quantum information techniques in a relativistic setting and on the other hand, provide a deeper understanding of the characterization of the inherent relativistic effects on the distribution of information.

References

[1] M. A. Nielsen, I. Chuang, "Quantum Computation and Quantum Information." Cambridge University, Cambridge (2000).

[2] M. Czachor, "Einstein-Podolsky-Rosen-Bohm experiment with relativistic massive particles." Physical Review A, **55** (1997) 77.

[3] R. M. Gingrich, C. Adami, "Quantum entanglement of moving bodies." Physical Review Letters, **89** (2002) 270402.

[4] D. C. M. Ostapchuk, R. B. Mann, "Generating entangled fermions by accelerated measurements on the vacuum." Physical Review A, **79** (2009) 042333.

[5] P. M. Alsing, I. Fuentes-Schuller, "Observer-dependent entanglement." Classical and Quantum Gravity, **29** (2012) 224001.

[6] J. L. M. Zepeda, J. Rueda Paz, M. Avila Aoki, S. H. Dong "Pentapartite Entanglement Measures of GHZ and W-Class State in the Noninertial Frame." Entropy, **24** (2022) 754.

[7] A. Belenchia, M. Carlesso. Bayraktar, D. Dequal, I. Derkach, G. Gasbarri, W. Herr, Y. L. Li, M. Rademacher, J. Sidhu, D. K. L. Oi, S. T. Seidel, R. Kaltenbaek, C. Marquardt, V. C. Usenko, L. Wrner, A. Xuereb, M. Paternostro, A. Bassi, "Quantum physics in space." Physics Reports, **951** (2022) 1.

[8] D. Cozzolino, B. Da Lio, D. Bacco, and L. K. Oxenløwe, "High-dimensional quantum communication: benefits, progress, and future challenges." Advanced Quantum Technologies, **2** (2019) 1900038.

[9] Luca Calderaro et al., "Towards quantum communication from global navigation satellite system." Quantum Science and Technology, **4** (2019) 015012.

[10] S. L. Braunstein and C. M. Caves.: Statistical distance and the geometry of quantum states. Physical Review Letters, **72** (1994) 3439.

[11] S. L. Braunstein, C. M. Caves, and G. J. Milburn, "Generalized uncertainty relations: Theory, examples, and Lorentz invariance." Annals of Physics (N.Y.) **247** (1996) 135.

[12] . Giovannetti, S. Lloyd, and L. Maccone, "Advances in quantum metrology." Nature Photonics, **5** (2011) 222.

[13] Y. Chen and H. Yuan, "Maximal quantum Fisher information matrix." New Journal of Physics, **19** (2017) 063023.

[14] K. Gietka, J. Chwedeczuk, T. Wasak, and F. Piazza, "Multipartite-Entanglement Dynamics in Regular-to-Ergodic Transition: a Quantum-Fisher-Information approach." Physical Review B, **99** (2019) 064303.

[15] J. Yao, "The effects of vacuum fluctuations on teleportation of quantum Fisher information. Scientific Reports, **7** (2017) 40193.

[16] M. Jafarzadeh, H. Rangani Jahromi, and M. Amniat Talab, "Teleportation of quantum resources and quantum Fisher information under Unruh effect." Quantum Information Processing, **17** (2018) 165.

[17] N. Metwally, "Unruh acceleration effect on the precision of parameter estimation." arXiv: 1609.02092 (2016).

[18] N. Metwally, "Estimation of teleported and gained parameters in a non-inertial frame." Laser Physics Letters, **14** (2017) 045202.

[19] G. Adesso, I. F. Schuller, M. Ericsson, "Continuous-variable entanglement sharing in noninertial frames." Physical Review A, **76** (2007) 062112.

[20] H. Lotfipour, S. Shahidani, R. Roknizadeh, M. H. Naderi, "Response of a mechanical oscillator in an optomechanical cavity driven by a finite-bandwidth squeezed vacuum excitation." Physical Review A, **93** (2016) 053827.

[21] M. D. Noia1, F. Giraldi, F. Petruccione, "Entanglement concentration for two-mode Gaussian states in non-inertial frames." Journal of Physics A: Mathematical and Theoretical, **50** 165302 (2017)

[22] D. Stoler, "Equivalence classes of minimum uncertainty packets." Physical Review D, **1** (1970) 3217.

[23] R. E. Slusher, L. W. Hollberg, B. Yurke, J. C. Mertz, J. F. Valley Slusher, "Observation of squeezed states generated by four-wave mixing in an optical cavity." Physical Review Letters, **55** (1985) 2409.

[24] F. Acernese et al. (Virgo Collaboration), "Increasing the astrophysical reach of the advanced Virgo detector via the application of squeezed vacuum states of light." Physical Review Letters, **123** (2019) 2331108.

[25] S. Davuluri and Y. Li, "Absolute rotation detection by Coriolis force measurement using optomechanics." New Journal of Physics, **18** (2016) 103047.

[26] L. Bai, L. Zhang, Y. Yang, R. Chang, Y. Qin, J. He, X. Wen, and J. Wang, "Enhancement of spin noise spectroscopy of rubidium atomic ensemble by using the polarization squeezed light." Optics Express, **30** (2022) 1925.

[27] A. M. Braczyk and T. C. Ralph, "Teleportation using squeezed single photons." Physical Review A, **78** (2008) 052304.

[28] Gerardo Adesso and Fabrizio Illuminati, "Entanglement in continuous-variable systems: recent advances and current perspectives." Journal of Physics A: Mathematical and Theoretical, **40** (2007) 7821.

[29] Gerardo Adesso, Sammy Ragy and Davide Girolami.: Continuous variable methods in relativistic quantum information: characterization of quantum and classical correlations of scalar field modes in noninertial frames. Classical and Quantum Gravity, **29** (2012) 224002.

[30] L. S. Costanzo et al., "Properties of hybrid entanglement between discrete- and continuous-variable states of light." Physica Scripta, **90** (2015) 074045.

[31] R. Pakniat, M. K. Tavassoly, M. H. Zandi, "Entanglement swapping and teleportation based on cavity QED method using the nonlinear atomfield interaction: Cavities with a hybrid of coherent and number states." Optics Communications, **382** (2017) 381.

[32] Rigas, J., Guhne, O., Lutkenhaus, N.: Entanglement verification for quantum-key-distribution systems with an underlying bipartite qubit-mode structure. Physical Review A, **73** (2006) 012341.

[33] S. W. Lee, H. Jeong, "Near-deterministic quantum teleportation and resource-efficient quantum computation using linear optics and hybrid qubits." Physical Review A, **87** (2013) 022326.

[34] H. Jeong, A. Zavatta, M. Kang, S. W. Lee, L. S. Costanzo, S. Grandi, T. C. Ralph, M. Bellini, "Generation of hybrid entanglement of light." Nature Photonics, **8** (2014) 564.

[35] O. Morin, K. Huang, J. Liu, H. L. Jeannic, C. Fabre, J. Laurat, "Remote creation of hybrid entanglement between particle-like and wave-like optical qubits. Nature Photonics, **8** (2014) 570.

[36] J. R. Glauber, "Coherent and incoherent states of the radiation field." Physical Review, **131** (1963) 2766.

[37] E. C. G. Sudarshan, "Equivalence of semiclassical and quantum mechanical descriptions of statistical light beams." Physical Review Letters, **10** (1963) 277.

[38] J. R. Klauder, "Continuous-representation theory. I. Postulates of continuous-representation theory." Journal of Mathematical Physics, **4** (1963) 1055.

[39] R. M. Wald.: Quantum Field Theory in Curved Spacetime and Black Hole Thermodynamics, University of Chicago Press, Chicago (1994).

[40] J. Liu, X. Jing, and X. Wang, "Phase-matching condition for enhancement of phase sensitivity in quantum metrology." Physical Review A, **88** (2013) 042316.

[41] Y. M. Zhang, X. W. Li, W. Yang, and G. R. Jin, "Quantum Fisher information of entangled coherent state in the presence of photon losses: exact solution." Physical Review A, **88** (2013) 043832.

[42] T. C. Ralph, G J Milburn, and T Downes, "Quantum connectivity of space-time and gravitationally induced decorrelation of entanglement." Physical Review A, **79** (2009) 22121.

[43] J. S. Sidhu, S. K. Joshi, M. Gundogan, T. Brougham, D. Lowndes, L. Mazzarella, M. Krutzik, S. Mohapatra, D. Dequal, G. Vallone, P. Villoresi, A. Ling, T. Jennewein, M. Mohageg, J. Rarity, I. Fuentes, S. Pirandola, D. K. L. Oi, "Advances in space quantum communications." (2021)

[44] D. Dequal et al., "Feasibility of satellite-to-ground continuous-variable quantum key distribution." npj Quantum Information, **7** (2021) 3.

[45] J. F. Fitzsimons, "Private quantum computation: an introduction to blind quantum computing and related protocols." npj Quantum Information, **3** (2017) 23.